Uncertainties of Temperature Measurements on Snow-Covered Land and Sea Ice from In Situ and MODIS Data during BROMEX

DOROTHY K. HALL

Cryospheric Sciences Laboratory, NASA Goddard Space Flight Center, Greenbelt, Maryland

SON V. NGHIEM

Jet Propulsion Laboratory, California Institute of Technology, Pasadena, California

IGNATIUS G. RIGOR

Polar Science Center, Applied Physics Laboratory, University of Washington, Seattle, Washington

JEFFREY A. MILLER

Cryospheric Sciences Laboratory, NASA Goddard Space Flight Center, Greenbelt, Maryland, and Wyle, Inc., Houston, Texas

(Manuscript received 10 July 2014, in final form 13 December 2014)

ABSTRACT

The Bromine, Ozone, and Mercury Experiment (BROMEX) was conducted in March and April of 2012 near Barrow, Alaska, to investigate impacts of Arctic sea ice reduction on chemical processes. During BROMEX, multiple sensors were deployed to measure air and surface temperature. The uncertainties in temperature measurement on snow-covered land and sea ice surfaces were examined using in situ data and temperature measurements that were derived from the Moderate Resolution Imaging Spectroradiometer (MODIS) and are part of the *Terra* and *Aqua* ice-surface temperature and land-surface temperature (LST) standard data products. Following an ~24-h cross-calibration study, two Thermochrons (small temperature-sensing devices) were deployed at each of three field sites: a sea ice site in the Chukchi Sea, a mixed-cover site, and a homogeneous tundra site. At each site, one Thermochron was shielded from direct sunlight and one was left unshielded, and they were placed on top of the snow or ice. The best agreement between the Thermochron- and MODIS-derived temperatures was found between the shielded Thermochrons and the *Aqua* MODIS LSTs, with an average agreement of 0.6° ± 2.0°C (sample size of 84) at the homogeneous tundra site. The results highlight some uncertainties associated with obtaining consistent air and surface temperature measurements in the harsh Arctic environment, using both in situ and satellite sensors. It is important to minimize uncertainties that could introduce biases in long-term temperature trends.

1. Introduction

Assessments of climate change show that the temperature in the Arctic has been changing by only a fraction of a degree Celsius in recent decades (Stocker et al. 2013). Thus, even small measurement errors can introduce temporal and spatial biases from which misleading conclusions may be drawn, highlighting the critical need for accurate and consistent temperature measurements in polar environments.

The Bromine, Ozone, and Mercury Experiment (BROMEX) field campaign was conducted in March and April of 2012 to investigate impacts of Arctic sea ice reduction on chemical processes, transport, and distribution of bromine, ozone, and mercury from snow-covered sea ice and land surfaces (Nghiem et al. 2013a,b; Moore et al. 2014). Temperature is a key factor in chemical reactions (Tarasick and Bottenheim 2002), and

Denotes Open Access content.

Corresponding author address: Dorothy K. Hall, Cryospheric Sciences Laboratory, NASA/GSFC, 8800 Greenbelt Rd., Greenbelt, MD 20771.
E-mail: dorothy.k.hall@nasa.gov

DOI: 10.1175/JAMC-D-14-0175.1

© 2015 American Meteorological Society

an increase in temperature fluctuations may lead to more episodes of the halogen chemical process known as bromine explosion (Wennberg 1999) and more-severe tropospheric ozone and mercury depletion in the Arctic (Nghiem et al. 2012). Therefore, temperature was measured both on the ground at selected field sites and from space during BROMEX.

The objectives of this work are 1) to investigate the uncertainties of measuring temperature on snow-covered land and sea ice during BROMEX by using surface temperatures that were derived from Maxim Integrated, Inc., Thermochrons (small temperature-sensing devices) and the Moderate Resolution Imaging Spectroradiometer (MODIS) and 2) to assess the accuracy of MODIS-derived surface temperatures by comparison with Thermochron-derived surface measurements. Here, we consider three Arctic domains that have different thermal characteristics: 1) snow-covered sea ice, 2) snow-covered tundra in a complex "built environment," defined as an area with human-made structures and energy-use networks, and 3) snow-covered tundra in a homogeneous environment.

Several different types of temperature sensors were used to collect an array of in situ temperature measurements during BROMEX. Meteorological stations were set up on sea ice and land, and drifting buoys were deployed as a part of the International Arctic Buoy Programme (IABP; Rigor et al. 2000, 2014). In addition, Thermochrons were placed directly on the snow or ice to record surface temperature. Thermochrons were particularly useful for this work because of their portability and their record of successful implementation in previous studies under Arctic conditions. The MODIS ice-surface temperature (IST) standard products from both the *Terra* and *Aqua* satellites (Hall et al. 2004) were used to obtain surface temperature over sea ice, and the MODIS land-surface temperature (LST) standard products (Wan et al. 2002) were used over the land sites (Hall et al. 2013).

2. Background

a. MODIS IST and LST standard data products

MODIS IST and LST are skin temperatures, or surface radiometric temperature (Dash et al. 2002), which is the temperature of the surface at radiative equilibrium at the interface between the snow/ice surface and the atmosphere. The estimated depth affecting the satellite-derived temperature is less than a few millimeters (Warren and Brandt 2008), but it can vary as the near-surface composition changes during the year. For example, if snow cover is present, its grain size and liquid water content will affect the dielectric properties and hence the penetration depth. The satellite swath-based IST and LST products were used in this work because swath products provide the time of the satellite overpass within ± 5 min. Knowledge of the acquisition time is needed to synchronize with ground observations.

We use the LST collection-5 standard product suite (MOD11 and MYD11) developed by Wan et al. (2002) and Wan (2008) with heritage from Wan and Dozier (1996). (MOD refers to a *Terra* MODIS standard product, and MYD refers to an *Aqua* MODIS standard product.) The MODIS 1-km-resolution LST algorithm produces a swath product (MOD/MYD11_L2) and is only available over land.

IST is mapped at 1-km resolution using the algorithm developed for the MODIS standard sea ice product, MOD/MYD29. We use collection-5 IST *Terra* and *Aqua* standard products. Detailed information on the MODIS IST product may be found in Hall et al. (2004) and Riggs et al. (2006) (and online at http://modis-snow-ice.gsfc.nasa.gov/?c5userguides). The MODIS IST algorithm derives its heritage from Key and Haefliger (1992) and Key et al. (1997). The MODIS IST is only available over sea ice and, as a special product, over the Greenland ice sheet (Hall et al. 2012).

There are similarities and differences in the algorithms that produce MOD/MYD11 and MOD/MYD29. Both employ a split-window technique using MODIS bands 31 (10.780–11.280 μm) and 32 (11.770–12.270 μm). The split-window method corrects for atmospheric effects on the basis of differential absorption in adjacent infrared (IR) bands and is widely used for atmospheric correction because the measured temperature difference between the two IR channels is proportional to the amount of water vapor in the atmosphere.

Although they produce similar results over snow and ice surfaces, the MOD/MYD29 IST algorithm uses a fixed snow/ice emissivity that is tuned to snow/ice targets, whereas the MOD11 LST algorithm estimates the emissivity on the basis of land cover type, atmospheric column water vapor, and lower-boundary air surface temperature. Thermal IR emissivity is insensitive to impurities, snow depth, liquid water content, and density (Warren 1982), although it is somewhat sensitive to grain size (Salisbury et al. 1994; Hori et al. 2006). Both the IST and LST algorithms use coefficients derived from MODIS spectral response functions and from regression analysis of radiative transfer simulations. In the MOD29 algorithm, sets of coefficients are implemented for different temperature ranges.

The cloud-mask standard product, MOD/MYD35, is used in both MOD/MYD11 and MOD/MYD29 but is handled differently in each algorithm. MOD/MYD11 interprets a pixel as clear if the cloud mask indicates 95% or greater probability of clear, whereas MOD/MYD29 interprets a pixel as clear if the cloud mask indicates 66% or greater probability of clear.

FIG. 1. Location map showing BROMEX field sites. Two Thermochrons were deployed at each field site. Thermochrons with blue, red, and yellow holders were deployed at the OOTI sea ice site, the NARL Hut 268 site, and the tundra snow site, respectively. (Photograph credit: the Polar Geospatial Center, University of Minnesota.)

b. *Thermochrons*

Thermochron sensors are small (16-mm diameter) digital thermometers and dataloggers that operate over a temperature range from −40° to +85°C. The Model DS1922L Thermochrons that are used in this work have an inherent accuracy that ranges from −0.8° to +1.5°C, according to the manufacturer's specifications, for temperatures from −40° to −10°C, which were the temperatures that were encountered during the BROMEX 2012 field work. Thermochrons have been used previously for measuring surface temperature of snow and ice (e.g., Lundquist and Lott 2008; Koenig and Hall 2010). Thermochrons used during a validation study in the 2009/10 winter at Summit, Greenland, were very accurate: they were within 0.1° ± 0.3°C of the National Oceanic and Atmospheric Administration (NOAA) temperature instrument for air temperatures in the range from −40° to −15°C (Koenig and Hall 2010). The same paper reported that LSTs from the MOD11_L2 (swath) product were ~3°C lower than Thermochron skin temperatures at Summit.

The NOAA temperature instrument at Summit has acquired 2-m air temperature data at the Temporary Atmospheric Watch Observatory since 2005 and is operated by the NOAA/Earth System Research Laboratory's Global Monitoring Division (http://www.esrl.noaa.gov/gmd/obop/sum/). It is actively ventilated and is serviced daily. This daily maintenance is important to reduce the presence of rime ice that can form on the instrument and affect the temperature retrievals. Because of the active ventilation and daily servicing, the accuracy of the NOAA temperature instrument is considered to be very high (Shuman et al. 2014).

Recent work performed at the Summit station by Shuman et al. (2014) shows that the offset between the NOAA temperature sensor, which senses ~2-m air temperature, and the MODIS *Terra*, or MOD29, IST is lowest near 0°C and increases as temperatures drop to −60°C. Although it is well known that near-surface air temperatures and surface temperatures do not necessarily agree (Miller 1956; Koenig and Hall 2010), the air and surface temperature patterns generally agree and provide great insight on the accuracy of the satellite-derived surface temperatures in a range of temperatures from 0° to ~−65°C, as discussed in Wenny et al. (2012). Thus, the calibration of MODIS *Terra* and *Aqua* bands 31 and 32 is best for snow/ice around 0°C (Wenny et al. 2012).

3. BROMEX field campaign and study area

BROMEX included participation and contributions from scientists, researchers, and support staff from 20 different agencies and institutions from the United States, Canada, Germany, and the United Kingdom in March and April of 2012. BROMEX also involved multiple satellite instruments, three aircraft, various field sites on sea ice and tundra, and meteorological buoys and stations. The field-study area included inland terrestrial sites and sea ice sites in the Beaufort and Chukchi Seas (Fig. 1). In addition to existing weather stations, a meteorological tower and a snow-measurement tower were installed by the field team at a site on the tundra to measure wind and temperature, along with snow. At these sites, continuous atmospheric chemical and meteorological measurements were made for about four weeks (Nghiem et al. 2013a,b). In addition, IABP buoys that were deployed offshore from the field camp and beyond

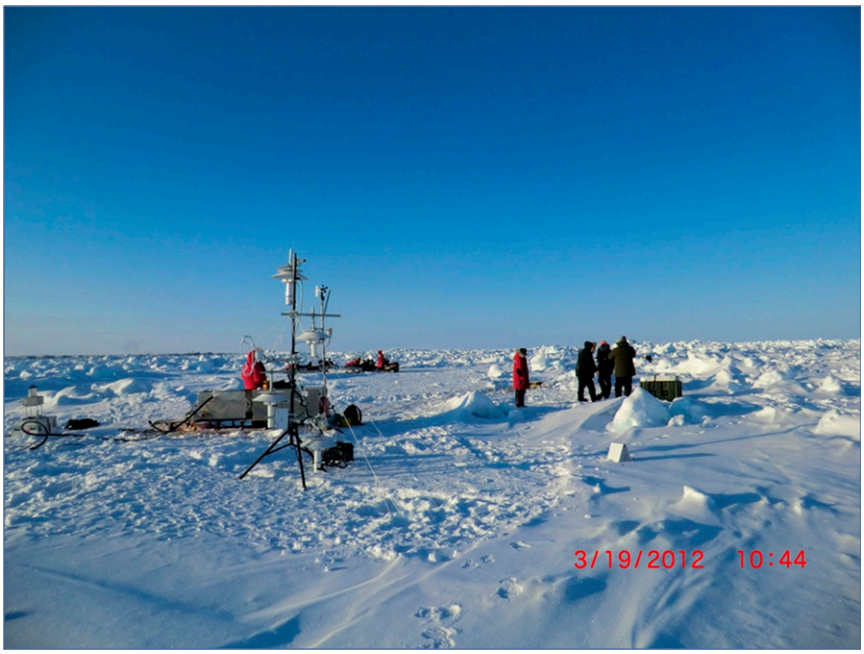

FIG. 2. OOTI sea ice site in the Chukchi Sea. The white notebook, referred to in the text, is shown in the foreground just to the right of center; the Thermochrons were deployed next to the white notebook as shown in the close-up view in Fig. 7, below.

provided measurements that are vital for large-scale analyses (Rigor et al. 2000).

During BROMEX the "Out On The Ice" (OOTI) sea ice site in the Chukchi Sea at 71°19′22.21″N and 156°44′38.79″W consisted of very rough, deformed first-year sea ice as far as the eye could see on a clear day (>1 km in all directions) (Fig. 2). Ridges between ice flows created many shadows on the sea ice surface. Snow depth averaging 11.6 ± 9.1 cm was measured around the sea ice site using a Cochranes of Oxford, Ltd., MagnaProbe.

The two study sites on land are located in and near Barrow, Alaska, which has been the site of intensive field work by scientists since at least the middle of the last century. Permafrost underlies all land surfaces at depths down to ~600 m and is composed of nearshore marine, fluvial, alluvial, and aeolian deposits. Forty percent of the surface is covered by large, elliptical thaw lakes, and drainage is poor (Brown et al. 1980). There is significant variation in thaw depth and near-surface soil moisture content, reflecting the influence of vegetation, substrate properties, snow-cover dynamics, and terrain. The region is underlain by silty soil, with drained lake basins and lagoons nearby (Hinkel and Nelson 2003). An inversion is present on 62% of winter days, with the day-to-day temperature changes being largely determined by changes in cloud cover (Dingman et al. 1980). Anticyclonic conditions during late winter lead to clear skies and allow receipt of a high percentage of the potential solar radiation.

For BROMEX, the Naval Arctic Research Laboratory (NARL) Hut 268 site located at 71°19′26.47″N and 156°41′8.03″W in Barrow was chosen for its complexity (Fig. 3). It is an inhomogeneous, mixed-use built-environment with a mix of natural environment and anthropogenic structures as far as could be seen (>1 km in all directions). Snow depth at this site was variable during BROMEX. At the location of the NARL Thermochron deployment, the snow depth was ~8 cm and rapidly changed to 40–60 cm at a distance of ~1 m toward a nearby dune.

The BROMEX tundra site was homogenous over a large area covering more than the 1 km × 1 km MODIS pixel area located at 71°16′30.45″N and 156°38′25.06″W. Photographs show extensive homogeneous snow-covered terrain that is virtually devoid of surface features for many kilometers, but with some very low topography (Fig. 4). The snow depth at this site was variable but averaged ~80 cm (with a standard deviation of 20%) according to snow-pit data that were acquired on 14 March 2012.

4. Method

The Thermochrons, placed approximately 3–6 cm apart, were cross calibrated at the NARL Hut 268 site in Barrow for ~24 h (Figs. 3 and 5) on 6–7 March 2012. Each Thermochron was placed in a holder that is 53 mm

FIG. 3. The site near NARL Hut 268, in an area that contains a mixture of built environment (huts, roads, power poles, etc.) and snow-covered tundra near the coast.

in length. They were unshielded and were in direct sunlight during daylight hours.

After the cross calibration was conducted, two Thermochrons were placed ~0.5 m apart on the snow/ice surface at each of the three sites: the OOTI sea ice site [Thermochrons 5 and 6 (blue holders)] from 19 March to 3 April (Fig. 2), near the NARL Hut 268 mixed-cover site [Thermochrons 7 and 8 (red holders)] during 13–31

FIG. 4. The tundra snow site in homogeneous land cover.

FIG. 5. Thermochrons outside of NARL Hut 268 on 6 Mar 2012 during cross calibration. The actual button-sized Thermochrons (16 mm in diameter) are not visible in this photograph because the colored holders (53 mm in length) block the view of the Thermochron from the camera. Thermochron 9 (see yellow holder on the left) was buried below the snow surface, and Thermochron 6 (see blue holder on the right) was partially buried. (Photograph credit: S. Nghiem.)

March (Fig. 3), and at the homogeneous tundra site [Thermochrons 9 and 10 (yellow holders)] during 9 March–5 April (Fig. 4). Although snow was dusted off of the Thermochron holders once daily, there were times during which snow accumulated on the surface of the holders between dustings. The effect of this snow on the accuracy of the Thermochron measurement is discussed later.

Each Thermochron was programmed to measure temperature once every 30 min during the BROMEX campaign. To ensure that comparisons with the satellite data were optimal, MODIS LST or IST retrievals were matched, within 30 min of the Thermochron measurements. In addition, only MODIS retrievals obtained from within 1 km of each of the sea ice or land sites were used. Each MODIS pixel of the LST or IST swath product is 1 km × 1 km at nadir (see box for scale in Fig. 1) and thus includes a large area of sea ice or land. See earlier discussion of the homogeneity of each of the three study sites.

5. Results

a. Cross calibration

In the ideal case, the temperatures measured by all of the Thermochrons would be exactly the same since they were separated by only a few centimeters at each location; there are some notable differences, however. The discrepancies during daytime may be due to different colors of holders (having different albedos), which may absorb differing amounts of solar radiation and cause differential heating of the handle and the sensor. In addition, unintended shielding of the sensor occurred as a result of a shadow being cast by a Thermochron handle. Each handle had a different angle with respect to the solar azimuth that changed diurnally. Snow cover on the Thermochron handles could also influence the temperature measurements because snow alters the effective albedo and thermal conductivity. These factors illustrate the difficulty in obtaining consistent temperature measurements, especially in the harsh Arctic environment.

Thermochrons 6 and 9 were partially and fully buried in the snow, respectively, as seen in Fig. 5. Note in Fig. 6 that those Thermochrons provide temperature readings that are different from the others during the cross-calibration study. Thermochron 9 provides higher temperatures at the beginning (~1.6°C) and end (~0.8°C) of the ~24-h study period, and Thermochron 6 readings are both higher *and* lower than most of the others. There are some reasons that this may have occurred: 1) snow cover on top insulated the Thermochrons, thus affecting the temperature reading; 2) the albedo difference due to the different colors of the holders may have influenced

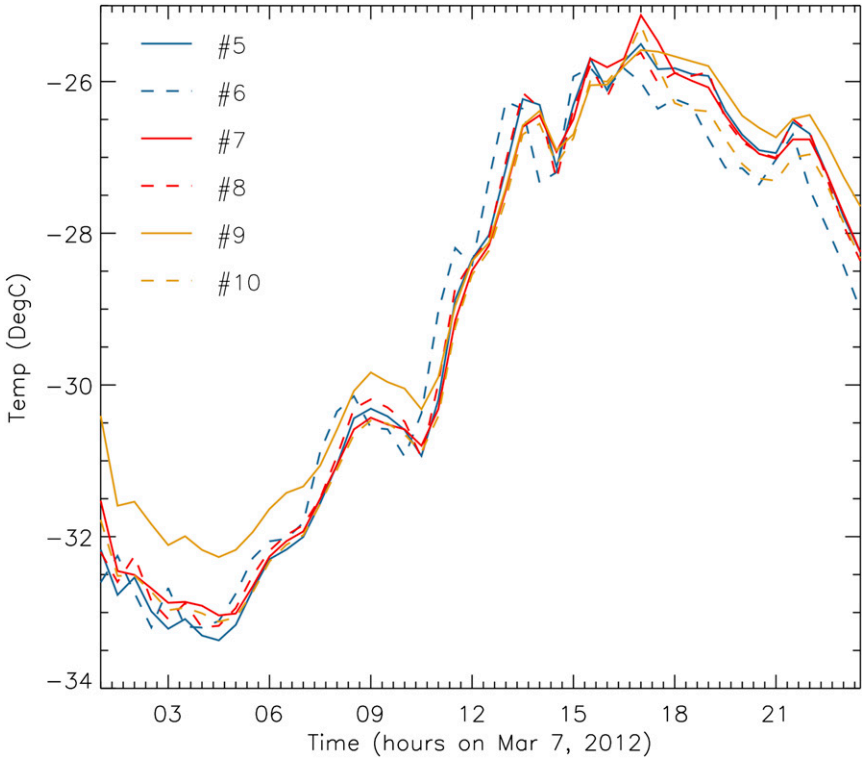

FIG. 6. Plots derived from the cross-calibration study outside of NARL Hut 268 (see Fig. 2) from 6 to 7 Mar 2012, showing the temperatures recorded by the Thermochrons. Six of these Thermochrons were later deployed at the field-study sites. Note the higher temperatures from Thermochron 9 at the beginning of the calibration study period and the higher temperatures from Thermochron 6 during the middle of the study period. All of these Thermochrons were in the direct sunlight during daylight hours.

heat absorption during the daylight hours; or 3) some combination of the above reasons. Although the other Thermochron holders are also brightly colored, they were not buried in the snow. Thermochrons 6 (deployed at the OOTI site) and 9 (deployed at the tundra snow site) did not show unusual behavior at those sites, as we will see later. Complexity from multiple effects and their interactions may explain why Thermochrons 6 and 9 show different temperature patterns from the other Thermochrons during cross calibration.

b. *Sea ice site*

The OOTI sea ice site (Nghiem et al. 2013b) had varied local microtopography that is due to the sea ice floes and the wind blowing snow onto the ice surface (see Fig. 2 and the GigaPan, Inc., hyperresolution panoramic imagery at http://gigapan.com/gigapans/101645). There was shadowing from even low ice ridges that affected the Thermochron temperature retrievals. Thermochrons 5 and 6 were deployed at this site. Thermochron 5 was shielded most of the time behind the white folder seen in Figs. 2 and 7.

Thermochron 6 was placed in direct sunlight, but because of microtopography there was a large amount of shadowing at the rough sea ice surface during daylight hours. This could explain why the shielded and unshielded Thermochrons generally provided similar temperatures at this site (Fig. 8), with Thermochron 5 (mostly shielded) measuring an average of 0.1° ± 2.3°C higher than Thermochron 6 (unshielded); most of the time they both behaved as if they were shielded, and the average difference between the shielded and unshielded Thermochrons is very small.

At the OOTI site, MODIS ISTs were lower than the corresponding shielded Thermochron temperatures: *Terra* IST was 4.0° ± 2.9°C (sample size $n = 46$) lower, and *Aqua* IST was 2.8° ± −4.3°C ($n = 50$) lower (Table 1). *Aqua* MODIS ISTs are a closer match to the Thermochron temperatures than are the *Terra* MODIS ISTs.

c. *NARL Hut 268 site*

Measurements from the mixed-cover site outside NARL Hut 268 provide a good example of the influence of Thermochron shielding (Fig. 9). Because of solar

FIG. 7. Thermochrons are shown on top of the sea ice in the Chukchi Sea. Thermochron 5 (on the left) was intentionally shielded behind the white notebook, and Thermochron 6 was in direct sunlight (on the right). Also see the locations of the Thermochrons and the white notebook in Fig. 2.

heating during daylight hours, the temperatures from the unshielded Thermochron 8 were higher (by up to 14.8°C) than were the temperatures from the shielded Thermochron 7. The average difference in shielded versus unshielded temperatures was 1.8° ± 2.8°C, with the temperatures of the shielded Thermochron (7) being lower, as expected. During darkness, in the absence of solar heating, temperatures from Thermochrons 7 and 8 matched well for most of the time. Effects of shading can affect in situ temperature measurement and can also vary with changes in insolation (at different times of the day and on different days of the month) and local meteorological conditions.

Note that on 25 March 2012 there was a closer correspondence during the daytime between the shielded and unshielded measurements than occurred during most of the other days of the study period (Fig. 9). We investigated the meteorological conditions for that day and found that thick plumes of near-surface vapor from leads in the sea ice were present (Fig. 10). These plumes of vapor prevented some solar radiation from reaching the ground, and therefore the unshielded Thermochron was acting more like a shielded Thermochron on that day and time.

At the NARL Hut 268 site, the MODIS-derived LSTs were lower than the shielded Thermochron temperatures, with the *Aqua* MODIS LSTs providing a closer match (0.9° ± 3.1°C; n = 18) to the Thermochron temperatures as compared with the *Terra* MODIS LSTs (2.9° ± 2.7°C; n = 33) (Table 1).

d. *Tundra snow site*

Thermochron 9 (Fig. 11) at the homogeneous tundra snow site was unshielded and in the direct sunlight and therefore recorded higher daytime temperatures for most of the study period (by 1.1° ± 3.1°C on average) as compared with the shielded Thermochron 10. The handle cast a shadow on Thermochron 9 early and late in the study period (between approximately 12 March and 2 April), causing temperature readings that are almost identical to the shielded Thermochron (see Fig. 10). The presence of the shadow was noted when viewing photos that had been acquired during the field work.

Because of shielding from direct solar radiation, Thermochron 10 provides a closer match with the MODIS LSTs. Relative to the MODIS-derived temperatures at this homogeneous tundra snow site, Thermochron temperatures were lower on average by 2.3° ± 3.9°C (n = 69) for *Terra* and slightly *higher* by 0.6° ± 2.0°C (n = 84) for *Aqua*. Data from the *Aqua* MODIS again provided a closer match than did data from the *Terra* MODIS.

6. Discussion and future work

Temperatures from the shielded Thermochrons (vs unshielded) provide a closer correspondence with the

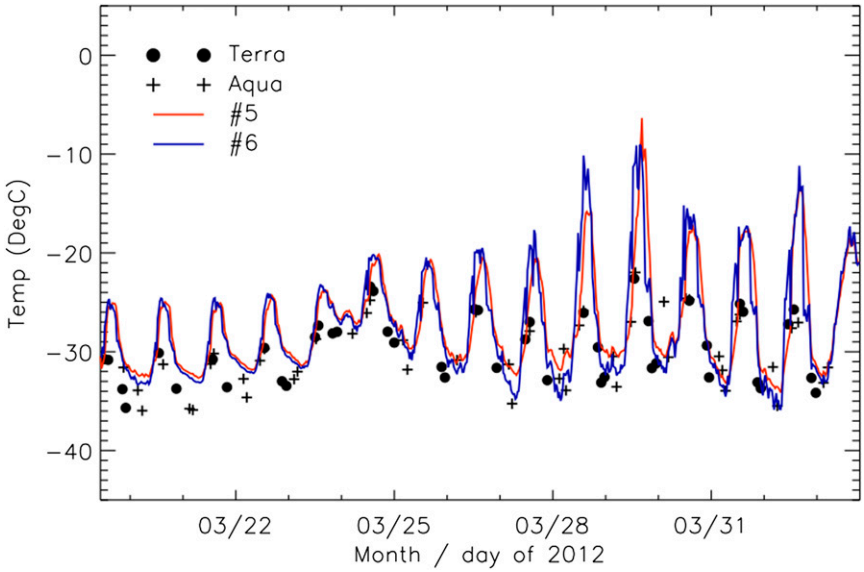

FIG. 8. OOTI sea ice site during 19 Mar–2 Apr 2012. Thermochron 5 was mostly shielded by the white notebook, and Thermochron 6 was placed in the direct sunlight (but affected by shadowing from microtopography). On average, temperatures from the mostly shielded Thermochron were 0.1° ± 2.3°C lower than those from the unshielded Thermochron. Also shown are MODIS *Terra* (n = 46) and *Aqua* (n = 50) ISTs acquired within 30 min of the Thermochron measurement. Note that there is some unavoidable overplotting of the *Terra* and *Aqua* ISTs that is due to close agreement.

MODIS LSTs and ISTs, as expected. This result is because satellite-derived surface temperature retrievals are not subject to some of the problems that plague in situ temperature sensors such as intense solar heating that can cause feedback from the surface when wind speed is low. Changes in insolation, shadowing, and surface snow may impact in situ sensors in a multitude of ways. Because these weather conditions and meteorological variables in the lowest layers of the atmosphere do not affect the stability of satellite sensors in space, the satellite-derived surface temperatures from clear-sky satellite retrievals can be more stable and more consistent than in situ sensors, making them potentially useful for development of long-term records. Satellite data are subject to inconsistencies relating to calibration and instrument degradation that can cause bias in the measurements, however. Therefore, the instrument calibration must be monitored closely throughout the lifetime of the sensor (e.g., Wenny et al. 2012). In addition, the clear-sky limitation introduces a cold bias in a time series of satellite observations because winter near-surface temperatures tend to be higher under cloudy conditions so that typically only the lower temperatures from clear days are recorded [as discussed in Hall et al. (2012)].

Surface temperatures derived from the *Aqua* MODIS products (MYD11 and MYD29) correspond more closely to the shielded Thermochrons than do the *Terra* surface temperatures (from the MOD11 and MOD29 products) (Table 1). The discrepancies between *Aqua* MODIS IST/LST and in situ Thermochron surface temperatures are less than 1.0°C when *Aqua* LSTs at the land sites are used and less than 3°C when *Aqua* ISTs at the sea ice site are used. Differences in the number of swaths used for *Terra* and *Aqua* and for the three sites are mainly due to varying cloud-cover conditions. Even within the same day, cloud conditions may vary, causing satellite swaths acquired from different times of the day to show different cloud conditions.

TABLE 1. Average difference between the *Aqua*- and *Terra*-derived surface temperatures and the shielded Thermochron-derived surface temperatures, or "ground truth," during BROMEX. The average difference in temperature is less using the *Aqua* MODIS, as discussed in the text. Here, n is the number of points.

Site (product)	*Aqua*	*Terra*
OOTI sea ice site (IST)	−2.8° ± 4.3°C (n = 50)	−4.0° ± 2.9°C (n = 46)
NARL Hut 268 tundra site (LST)	−0.9° ± 3.1°C (n = 33)	−2.9° ± 2.7°C (n = 18)
Homogeneous tundra site (LST)	0.6° ± 2.0°C (n = 84)	−2.3° ± 3.9°C (n = 69)

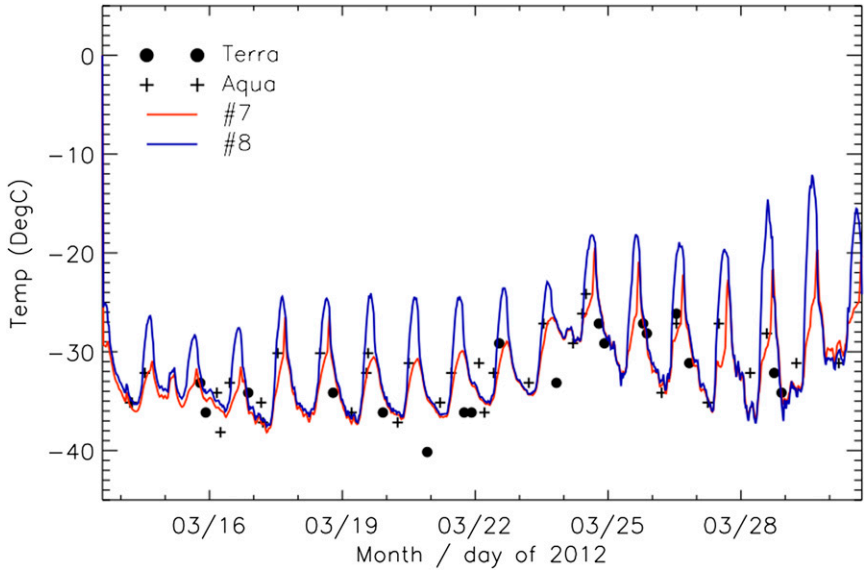

FIG. 9. NARL Hut 268 site. Thermochron 7 was shielded and is therefore not in direct sunlight, and Thermochron 8 was unshielded and in direct sunlight. On average, temperatures from the shielded Thermochron were 1.8° ± 2.8°C lower than those from the unshielded Thermochron. Also shown are MODIS *Terra* ($n = 18$) and *Aqua* ($n = 33$) LSTs acquired within 30 min of the Thermochron measurements. Note that there is some unavoidable overplotting of the *Terra* and *Aqua* LSTs that is due to close agreement.

Aqua MODIS bands have a lower saturation temperature (~340 K) than do the *Terra* bands (~380 K), and lower saturation or smaller dynamic range means better resolution; thus, the *Aqua* MODIS is able to measure lower temperatures more accurately, perhaps explaining why *Aqua* MODIS surface temperatures are consistently a closer match with the Thermochron temperatures [MODIS Characterization and Support Team (MCST) 2014, personal communications].

FIG. 10. Plumes of vapor emanating from leads in the sea ice on 25 Mar 2012.

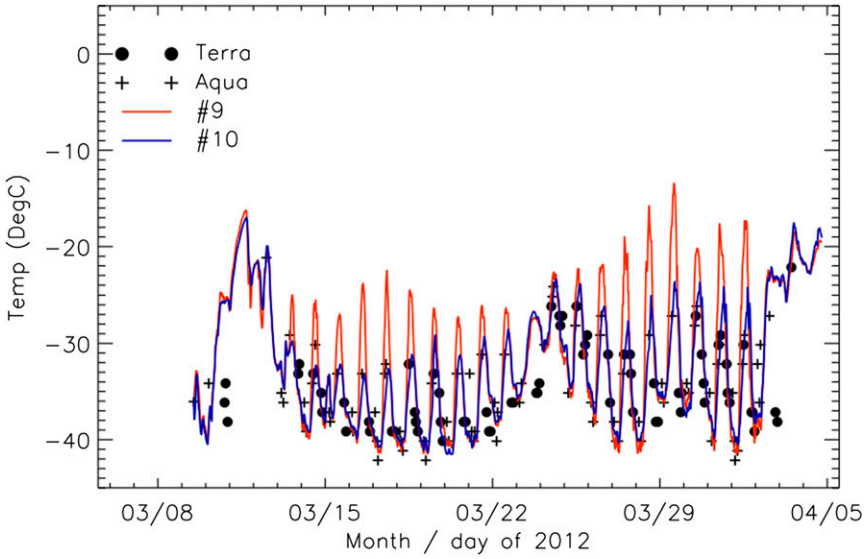

FIG. 11. Tundra snow site. Thermochron 10 was shielded, and Thermochron 9 was unshielded and in direct sunlight. On average, temperatures from the shielded Thermochron were 1.1° ± 3.1°C lower than those from the unshielded Thermochron. Also shown are MODIS *Terra* (n = 69) and *Aqua* (n = 84) LSTs acquired within 30 min of the Thermochron measurement. Note that there is some unavoidable overplotting of the *Terra* and *Aqua* LSTs that is due to close agreement.

Comparing a point measurement with a 1 km × 1 km measurement (MODIS footprint at nadir) is problematic and is likely responsible for some of the differences between the Thermochron and MODIS measurements, as discussed in prior work (e.g., Hall et al. 2008). For BROMEX the Thermochron-derived temperatures were generally higher than the MODIS-derived temperatures.

A "point measurement" derived from a Thermochron might not be representative of the 1 km × 1 km study site of the MODIS pixel as discussed in Section 3. That is particularly true at a site where there is mixed cover that includes some buildings. Exposed rocks (and trees) within a pixel may be much warmer than the snow and the radiation emitted from these surfaces, especially in the spring, and this tends to inflate the satellite-measured temperatures (Dozier and Warren 1982). We are confident, however, that our homogeneous tundra site outside of Barrow (Fig. 1) is representative of the surrounding area as a 3 pixel × 3 pixel area surrounding the tundra study site provided LSTs with a low standard deviation. For example, a temperature of −21.3° ± 0.1°C was retrieved from the *Aqua* MODIS LST for a scene acquired on 10 March 2012. On other days the range in standard deviation was 0.1°–0.6°C but was typically less than 0.5°C.

Diurnal differences may affect satellite and in situ temperature measurements in different ways because of differences in insolation and local weather conditions. Furthermore, the Thermochron retrievals are influenced by snow on the surfaces of the handles. It was difficult to keep the Thermochrons swept free of snow at all times because they were dusted only once daily.

Our results suggest that data from automated temperature sensors installed in the Arctic that are unattended and without routine maintenance may need to be reanalyzed to assess their accuracy. There are many environmental and other effects that affect the measurements, such as rime ice that can form on an instrument or a covering of snow that can provide insulation between the air and snow temperatures. Some of these issues are more important during daylight hours.

Given a wide array of different types of sensors, made of different materials and having different-colored housings, there is a need for the international science community to initiate discussions about development of protocols for measuring air and surface temperatures in the harsh environment of the Arctic, which drastically differs from benign laboratory conditions. Furthermore, specifications from the manufacturers of the sensors should not be taken as the final accuracy, regardless of whether such specifications were derived following National Institute of Standards and Technology standards under strictly controlled laboratory environments because those sensors are exposed to extreme weather and wide variability that are not controllable as they are in a laboratory.

As motivated by the findings from BROMEX, in future work it would be very useful to do a controlled analysis of Thermochrons having different-colored

handles that are placed on top of the snow. Results from such an analysis should answer any outstanding questions about the influence of the color of the holder on the temperature retrieval.

7. Summary and conclusions

First, we cross calibrated the Thermochrons. Some differences in derived daytime temperatures were identified and were thought possibly to be due to different-colored holders absorbing different amounts of solar radiation, unintended shielding such as from the effect of a shadow being cast by the handle of the Thermochron holder, and snow overlying the Thermochron sensors. At the field sites, the best correspondence between the MODIS and shielded Thermochron temperatures was found at the homogeneous tundra site where the MODIS *Aqua* LST was 0.6° ± 2.0°C lower than the temperature of the shielded Thermochron. The poorest correspondence was found at the OOTI sea ice site, where the MODIS IST from the *Terra* satellite was 4.0° ± 2.9°C lower than the temperature of the shielded Thermochron. A large amount of small-scale topographic variability and shadowing on the sea ice surface contributed to difficulties in measuring surface temperature accurately over sea ice.

Calibration of MODIS IR bands at the very cold temperatures characteristic of BROMEX is less accurate than at higher temperatures (near 0°C) (Wenny et al. 2012; Shuman et al. 2014). The closer correspondence in temperature between the *Aqua* MODIS and Thermochrons versus the *Terra* MODIS and Thermochrons is likely explained by the smaller dynamic range of the *Aqua* sensor in comparison with that of the *Terra* sensor (Wenny et al. 2012; MCST 2014, personal communications).

Factors such as unintended shielding of the Thermochrons, specific placement with respect to the position of the handle, and microtopography of the sea ice surface were documented to affect surface temperature retrievals by the Thermochrons, and the color of the Thermochron holder was also suspected of affecting the surface temperature retrievals. Therefore, regardless of how manufacturers determine sensor accuracies in strictly controlled laboratory conditions, a protocol for measuring air and surface temperature is needed for Arctic conditions so as to achieve accuracy and consistency.

Accuracy of temperature measurements is of the utmost importance for climate-change studies. Biases caused by measurement error can lead to erroneous conclusions about regional climate change. Satellite sensors, unaffected by near-surface weather conditions, can provide the accuracy and consistency that is needed for long-term climate studies, but there is a clear-sky bias when a time series of satellite measurements is used, and the calibration of the satellite instruments needs to be continually monitored for stability. This work highlights difficulties in measuring and validating skin temperature in a polar environment, using both in situ and satellite instruments.

Acknowledgments. The research carried out at the National Aeronautics and Space Administration (NASA) Goddard Space Flight Center (GSFC) and at the Jet Propulsion Laboratory, California Institute of Technology, was supported by the NASA Cryospheric Sciences Program. Author I. Rigor is funded by NASA and other contributors to the U.S. Interagency Arctic Buoy Program. We thank Jody Hoon-Starr for programming help, Paul Morin from the University of Minnesota for high-resolution imagery, and Chris Linder of the University of Washington for the GigaPan photography. We also thank Christopher Shuman of NASA and the University of Maryland, Baltimore County, Joint Center for Earth Systems Technology and Brian Wenny and Jack Xiong of the MCST at NASA/GSFC for discussions about MODIS sensor calibration. In addition, we thank the UMIAQ Company, the Barrow whaling community, and the Barrow Arctic Science Consortium for their assistance during BROMEX.

REFERENCES

Brown, J., P. C. Miller, L. L. Tieszen, and F. L. Bunnell, 1980: *An Arctic Ecosystem: The Coastal Tundra at Barrow, Alaska.* US/IBP Synthesis Series, Vol. 12, Dowden, Hutchinson and Ross, 571 pp.

Dash, P., F.-M. Göttsche, F.-S. Olesen, and H. Fischer, 2002: Land surface temperature and emissivity estimation from passive sensor data: Theory and practice—Current trends. *Int. J. Remote Sens.,* **23,** 2563–2594, doi:10.1080/01431160110115041.

Dingman, S. L., R. G. Barry, G. Weller, C. Benson, E. F. LeDrew, and C. W. Goodwin, 1980: Climate, snow cover, microclimate, and hydrology. *An Arctic Ecosystem: The Coastal Tundra at Barrow, Alaska,* J. Brown et al., Eds., U.S./IBP Synthesis Series, Vol. 12, Dowden, Hutchinson and Ross, 30–65.

Dozier, J., and S. C. Warren, 1982: Effect of viewing angle on the infrared brightness temperature of snow. *Water Resour. Res.,* **18,** 1424–1434, doi:10.1029/WR018i005p01424.

Hall, D. K., J. Key, K. A. Casey, G. A. Riggs, and D. J. Cavalieri, 2004: Sea ice surface temperature product from the Moderate Resolution Imaging Spectroradiometer (MODIS). *IEEE Trans. Geosci. Remote Sens.,* **42,** 1076–1087, doi:10.1109/TGRS.2004.825587.

——, J. E. Box, K. A. Casey, S. J. Hook, C. A. Shuman, and K. Steffen, 2008: Comparison of satellite-derived ice and snow surface temperatures over Greenland from MODIS, ASTER, ETM+ and in-situ observations. *Remote Sens. Environ.,* **112,** 3739–3749, doi:10.1016/j.rse.2008.05.007.

——, J. C. Comiso, N. E. DiGirolamo, C. A. Shuman, J. R. Key, and L. S. Koenig, 2012: A satellite-derived climate-quality data record of the clear-sky surface temperature of the

Greenland Ice Sheet. *J. Climate,* **25,** 4785–4798, doi:10.1175/JCLI-D-11-00365.1.

——, S. G. Nghiem, and I. Rigor, 2013: Evaluation of surface temperature measurements during BROMEX 2012. *Proc. 15th Conf. on Atmospheric Chemistry,* Austin, TX, Amer. Meteor. Soc., 646. [Available online at https://ams.confex.com/ams/93Annual/webprogram/Paper211944.html.]

Hinkel, K. M., and F. E. Nelson, 2003: Spatial and temporal patterns of active layer thickness at Circumpolar Active Layer Monitoring (CALM) sites in northern Alaska, 1995–2000. *J. Geophys. Res.,* **108,** 8168, doi:10.1029/2001JD000927.

Hori, M., and Coauthors, 2006: In-situ measured spectral directional emissivity of snow and ice in the 8–14 μm atmospheric window. *Remote Sens. Environ.,* **100,** 486–502, doi:10.1016/j.rse.2005.11.001.

Key, J., and M. Haefliger, 1992: Arctic ice surface temperature retrieval from AVHRR thermal channels. *J. Geophys. Res.,* **97,** 5885–5893, doi:10.1029/92JD00348.

——, J. Collins, C. Fowler, and R. S. Stone, 1997: High-latitude surface temperature estimates from thermal satellite data. *Remote Sens. Environ.,* **61,** 302–309, doi:10.1016/S0034-4257(97)89497-7.

Koenig, L. S., and D. K. Hall, 2010: Comparison of satellite, Thermochron and station temperatures at Summit, Greenland, during the winter of 2008/09. *J. Glaciol.,* **56,** 735–741, doi:10.3189/002214310793146269.

Lundquist, J. D., and F. Lott, 2008: Using inexpensive temperature sensors to monitor the duration and heterogeneity of snow-covered areas. *Water Resour. Res.,* **44,** W00D16, doi:10.1029/2008WR007035.

Miller, D. H., 1956: The influence of snow cover on local climate in Greenland. *J. Meteor.,* **13,** 112–120, doi:10.1175/1520-0469(1956)013<0112:TIOSCO>2.0.CO;2.

Moore, C. W., D. Obrist, A. Steffen, R. M. Staebler, T. A. Douglas, A. Richter, and S. V. Nghiem, 2014: Convective forcing of mercury and ozone in the Arctic boundary layer induced by leads in sea ice. *Nature,* **506,** 81–84, doi:10.1038/nature12924.

Nghiem, S. V., and Coauthors, 2012: Field and satellite observations of the formation and distribution of Arctic atmospheric bromine above a rejuvenated sea ice cover. *J. Geophys. Res.,* **117,** D00S05, doi:10.1029/2011JD016268.

——, and Coauthors, 2013a: Arctic sea ice reduction and tropospheric chemical processes. *Proc. Bionature 2013: Fourth Int. Conf. on Bioenvironment, Biodiversity and Renewable Energies,* Lisbon, Portugal, International Academy, Research and Industry Association, 4–8.

——, and Coauthors, 2013b: Studying bromine, ozone, and mercury chemistry in the Arctic. *Eos, Trans. Amer. Geophys. Union,* **94,** 289–291, doi:10.1002/2013EO330002.

Riggs, G. A., D. K. Hall, and V. V. Salomonson, 2006: MODIS snow products user guide. NASA Goddard Space Flight Center Rep., 80 pp. [Available online at http://modis-snow-ice.gsfc.nasa.gov/uploads/sug_c5.pdf.]

Rigor, I., R. L. Colony, and S. Martin, 2000: Variations in surface air temperature observations in the Arctic, 1979–97. *J. Climate,* **13,** 896–914, doi:10.1175/1520-0442(2000)013<0896:VISATO>2.0.CO;2.

——, and Coauthors, 2014: Arctic Observing Experiment—An assessment of instruments used to monitor the polar environments. *2010 Fall Meeting,* San Francisco, CA, Amer. Geophys. Union, Abstract C31D-0346.

Salisbury, J. W., D. M. D'Aria, and A. Wald, 1994: Measurements of thermal infrared spectral reflectance of frost, snow, and ice. *J. Geophys. Res.,* **99,** 24 235–24 240, doi:10.1029/94JB00579.

Shuman, C. A., D. K. Hall, N. E. DiGirolamo, T. K. Mefford, and M. J. Schnaubelt, 2014: Comparison of near-surface air temperatures and MODIS ice-surface temperatures at Summit, Greenland (2008–13). *J. Appl. Meteor. Climatol.,* **53,** 2171–2180, doi:10.1175/JAMC-D-14-0023.1.

Stocker, T. F., and Coauthors, 2013: *Climate Change 2013: The Physical Science Basis.* Cambridge University Press, 1535 pp. [Available online at http://www.climatechange2013.org/images/report/WG1AR5_ALL_FINAL.pdf.]

Tarasick, D. W., and J. W. Bottenheim, 2002: Surface ozone depletion episodes in the Arctic and Antarctic from historical ozonesonde records. *Atmos. Chem. Phys.,* **2,** 197–205, doi:10.5194/acp-2-197-2002.

Wan, Z., 2008: New refinements and validation of the MODIS land-surface temperature/emissivity products. *Remote Sens. Environ.,* **112,** 59–74, doi:10.1016/j.rse.2006.06.026.

——, and J. Dozier, 1996: A generalized split-window algorithm for retrieving land-surface temperature from space. *IEEE Trans. Geosci. Remote Sens.,* **34,** 892–905, doi:10.1109/36.508406.

——, Y. Zhang, Q. Zhang, and Z.-L. Li, 2002: Validation of the land-surface temperature products retrieved from *Terra* Moderate Resolution Imaging Spectroradiometer data. *Remote Sens. Environ.,* **83,** 163–180, doi:10.1016/S0034-4257(02)00093-7.

Warren, S. G., 1982: Optical properties of snow. *Rev. Geophys. Space Phys.,* **20,** 67–89, doi:10.1029/RG020i001p00067.

——, and R. E. Brandt, 2008: Optical constants of ice from the ultraviolet to the microwave: A revised compilation. *J. Geophys. Res.,* **113,** D14220, doi:10.1029/2007JD009744.

Wennberg, P., 1999: Atmospheric chemistry: Bromine explosion. *Nature,* **397,** 299–301, doi:10.1038/16805.

Wenny, B. N., X. Xiong, and S. Madhavan, 2012: Evaluation of *Terra* and *Aqua* MODIS thermal emissive band calibration consistency. *Sensors, Systems, and Next-Generation Satellites XVI,* R. Meynart, S. P. Neeck, and H. Shimoda, Eds., International Society for Optical Engineering (SPIE Proceedings, Vol. 8533), doi:10.1117/12.974230.